4232–4244 *Nucleic Acids Research, 2006, Vol. 34, No. 15* *Published online 25 August 2006*
doi:10.1093/nar/gkl451

SURVEY AND SUMMARY

DNA mechanics as a tool to probe helicase and translocase activity

Timothée Lionnet[1,2], Alexandre Dawid[2,3], Sarah Bigot[4], François-Xavier Barre[4,5], Omar A. Saleh[1,2], François Heslot[2,3], Jean-François Allemand[1,2], David Bensimon[1,2] and Vincent Croquette[1,2,*]

[1]Laboratoire de Physique Statistique de l' Ecole Normale Supérieure, UMR 8550 CNRS, 24 rue Lhomond, 75231 Paris Cedex 05, France, [2]Département de Biologie, Ecole Normale Supérieure, 46 rue d'Ulm, 75231 Paris Cedex, 05, France, [3]Laboratoire Pierre Aigrain, Ecole Normale Supérieure, UMR 8551 CNRS, 24 rue Lhomond, 75231 Paris Cedex 05, France, [4]Laboratoire de Microbiologie et de Génétique Moléculaire, CNRS UMR5100, Toulouse, France and [5]Centre de Génétique Moléculaire, CNRS UPR2167, Gif-sur-Yvette, France

Received March 31, 2006; Revised June 6, 2006; Accepted June 12, 2006

ABSTRACT

Helicases and translocases are proteins that use the energy derived from ATP hydrolysis to move along or pump nucleic acid substrates. Single molecule manipulation has proved to be a powerful tool to investigate the mechanochemistry of these motors. Here we first describe the basic mechanical properties of DNA unraveled by single molecule manipulation techniques. Then we demonstrate how the knowledge of these properties has been used to design single molecule assays to address the enzymatic mechanisms of different translocases. We report on four single molecule manipulation systems addressing the mechanism of different helicases using specifically designed DNA substrates: UvrD enzyme activity detection on a stretched nicked DNA molecule, HCV NS3 helicase unwinding of a RNA hairpin under tension, the observation of RecBCD helicase/nuclease forward and backward motion, and T7 gp4 helicase mediated opening of a synthetic DNA replication fork. We then discuss experiments on two dsDNA translocases: the RuvAB motor studied on its natural substrate, the Holliday junction, and the chromosome-segregation motor FtsK, showing its unusual coupling to DNA supercoiling.

INTRODUCTION

Helicases and DNA translocases are motors that move along or pump DNA by converting the energy from NTP (or dNTP) hydrolysis into mechanical work (1–4). The amount of energy available from one such reaction, under physiological conditions, is about 20 k_BT (k_B is Boltzmann's constant and $T \sim 300$ K at room temperature; 20 $k_BT \sim 8 \times 10^{-20}$ J $\sim$ 80 pN.nm $\sim$ 12 kcal/mol). The distance traveled by these motors during an enzymatic cycle is a few base pairs ($\sim$1 nm); thus, at 100% efficiency, the motors can generate maximum forces of tens of picoNewtons.

How these translocases convert the chemical energy derived from ATP hydrolysis into mechanical work is a question that has been addressed through various single molecule techniques. Fluorescence techniques, such as FRET, allow one to detect and measure translocase activity at the single molecule level (5–10), see also the review by Rasnik *et al*. in this issue (11). In addition, numerous single molecule manipulation methods have been developed, such as tethered particle motion (TPM) (12–14), atomic force microscopy (15), biomembrane force probe (16), glass microfiber manipulation (17,18), flow induced force (9), optical (19) and magnetic tweezers (20) [see (21,22) and references therein].

Using these methods (except the TPM) one can apply a picoNewton force on the motor or its DNA substrate. Single-particle tracking offers nanometer resolution of the changes in DNA length (or enzyme position) resulting from translocase activity, thus allowing real-time detection of enzymatic dynamics (23–31). Exerting a force on the DNA substrate has two major advantages: first, it straightens the otherwise coiled DNA molecule, simplifying the detection of the motor on its track. Second, the force can be used as an additional thermodynamic parameter: its influence on the enzymatic activity yields information on the kinetics and thermodynamics of the process (32).

*To whom correspondence should be addressed at Laboratoire de Physique Statisque de l' Ecole Normale Supérieure, 24 rue Lhomond, 75005 Paris, France. Tel: 33 1 44 32 34 92; Fax: 33 1 44 32 34 33; Email: Vincent.Croquette@lps.ens.fr
Present address:
Omar A. Saleh, Materials Department, University of California, Santa Barbara, CA 93106, USA

In this review we shall focus on single molecule manipulation techniques, which provide a simple and convenient means to stretch and/or twist a single DNA molecule while measuring its end-to-end extension. We shall describe how micromanipulation techniques can be used to determine a variety of mechanical properties of DNA: the elasticity of single- and double-stranded DNA (dsDNA), and the properties of supercoiled DNA. Knowledge of these properties will then be used as a tool to track the interactions of various molecular motors with DNA. Different examples will be developed here: first, the observation of four different helicases: UvrD, NS3, RecBCD and gp4; and second, experiments on the translocases RuvAB and FtsK.

MICROMANIPULATION TECHNIQUES AND MECHANICAL PROPERTIES OF DNA

While several different micromanipulation techniques exist, we shall here only describe three which have actually been used to probe helicase and translocase activity: flow induced DNA stretching, optical tweezers and magnetic tweezers.

It is possible to specifically tether a micron sized bead by a single DNA molecule to the glass surface of a microscope sample. By flushing solution into the experiment chamber at a controlled rate one can exert a constant drag force in the 1–10 pN range (33), (Figure 1A), sufficient to stretch the DNA molecule. Video tracking of the horizontal bead position provides the DNA molecule length.

Optical tweezers are obtained by focusing a strong laser beam into a water solution thus efficiently trapping any micron sized bead whose refractive index is higher than that of water (Figure 1B). The bead is then held in the trap by a virtual spring, which can be calibrated using different methods (19,34), to yield a typical stiffness 0.1 $pN.nm^{-1}$.

The basic principle of a magnetic trap is to attach one end of a DNA molecule to a glass substrate and the other end to a magnetic bead (Figure 1C). Two nearby external magnets produce a strong magnetic field gradient that attracts the bead, creating a vertical stretching force whose magnitude is controlled by the distance between the magnets and the sample. By monitoring the 3D position of the bead in real-time using video microscopy, it is possible to determine the stretching force (22) and the molecule's extension with nanometer resolution at a typical rate of 60 frames/s. If one rotates the magnets while keeping the bead-magnets distance constant, the DNA molecule twists, provided the molecule does not contain nicks, and is attached by several bonds at each extremity.

dsDNA elasticity

The double helix structure of DNA makes it, locally, a very stiff molecule with base pairs stacked in a highly ordered manner. However, DNA molecules are very long polymers that adopt in solution a fluctuating coiled structure with large bending radii and an average zero end-to-end distance. Applying a force to both ends of a DNA molecule stretches it to a finite extension. The force-extension behavior of DNA is well described by the worm-like chain model of polymer theory (35,36), which depends on two parameters: the molecule's contour length L and its persistence length P (typically ~50 nm). The persistence length P is a measurement of DNA's bending stiffness: it is the length over which thermal fluctuations will typically bend the molecule by 1 radian. The elasticity curve (Figure 2) displays a highly non-linear behavior: below 5 pN, the force is used to straighten the fluctuating coil along the force axis. Above 5 pN, the molecule stretches like a regular spring and undergoes a transition to a new overstretched structure at 65 pN (37).

ssDNA elasticity

In contrast with dsDNA, ssDNA is a far more flexible polymer, creating a much tighter random coil configuration that leads to strong intramolecular interactions; further, ssDNA presents unpaired bases, which can bind both locally, to create hairpins, or with distal regions, creating complex higher-order structures. As a result, at low force an ssDNA contains numerous weak intramolecular bonds, and forms a small coil with a very short end-to-end extension (37). Interestingly, this intramolecular base pairing has the consequence that two ssDNA molecules with identical contour lengths, but different sequences, will usually have different low force elasticity curves (38). In the opposite limit,

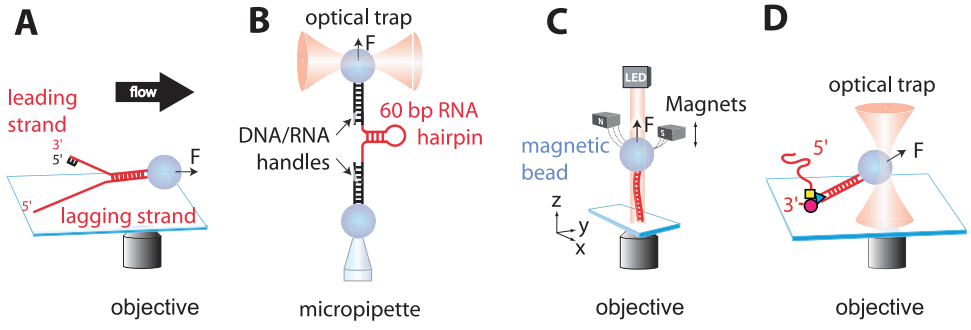

Figure 1. Various micromanipulation Set-ups. (**A**) Flow cell Set-up used in the study of the T7 replication fork (33). The DNA fork is tethered on the bottom of the flow cell and on a bead by respectively its lagging strand and duplex end. (**B**) Optical tweezers Set-up. A DNA/RNA hybrid molecule containing the RNA hairpin of interest is tethered between an optically trapped bead and a bead held in a micropipette by suction (26). (**C**) Magnetic tweezers set-up (20). A DNA molecule is anchored at one end to a micron sized magnetic bead and at the other to the bottom surface of a square glass capillary tube, which is placed on top of a microscope objective. Small magnets placed above the sample can be used to pull and twist the DNA molecule. (**D**) Set-up used for the RecBCD study (24). The biotin-labeled RecBCD helicase is bound to the surface of the chamber. The enzyme binds DNA which distal end is specifically bound to a bead held in an optical trap.

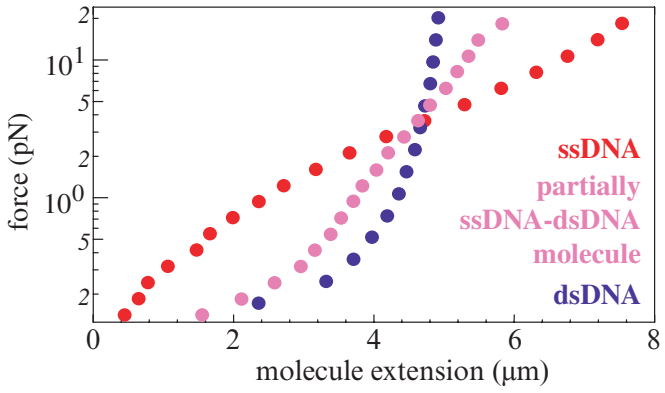

Figure 2. Elasticity curves of the same DNA molecule in its double-stranded form, single-stranded form, and in a mixture of both. Despite having the same number of nucleotides, the extension of ssDNA is shorter than dsDNA for F < 5 pN, while it becomes larger above. Adapted from (73).

where the stretching force is strong enough to disrupt the base pairing, ssDNA extends considerably more than its double-stranded more rigid counterpart, possibly twice as much. Both ss- and dsDNA have the same extension at a force of about 5 pN.

Unzipping dsDNA

An experiment on dsDNA was performed in 1997 in which a micro-needle was used to pull apart the strands of a dsDNA while monitoring the opening force (39). This process, the mechanical conversion of dsDNA to two unpaired ssDNA, resembles closely what is achieved by a helicase. The force necessary to separate the two strands is directly related to the binding energy of the Watson–Crick base pair. Typically, 10–15 pN are required to open up the molecule for a generic DNA substrate; the force rises with the GC content of the molecule and is larger for an RNA substrate (15–20 pN). This experiment has also been performed with magnetic tweezers in a constant force regime by Prentiss *et al.* (40). Such an unzipping geometry provides a very simple way of recording helicase activity, as demonstrated below for the study of NS3 helicase.

Supercoiling a single dsDNA molecule

While in many biological situations, it is not clear if force plays a role, torsional stress is often a relevant variable. Many enzymes regulate, or are regulated by, the torsional state of dsDNA (note that ssDNA is always torsionally unconstrained since it can rotate freely around the bonds in the sugar-phophate backbone). Torsional stress is physically described using two conjugate variables: the torque and angular displacement around the molecule's axis (just as the linear elastic state is described using the force and extension variables). In a biological context, the magnitude of torsional stress is referred to as the amount of supercoiling, a quantity proportional to the angular displacement.

Magnetic tweezers offer a simple means to directly control the supercoiled state of a DNA molecule. If the DNA molecule does not contains any nicks, and if the attachment at each end is made by multiple bonds, then rotating the bead around the vertical axis will twist the DNA molecule. This is simply accomplished by rotating the magnets around the vertical axis while keeping the distance between the magnets and the sample constant. In this process, the force applied to the DNA molecule is constant while the twist absorbed by the DNA is equal to the number of turns made by the magnets.

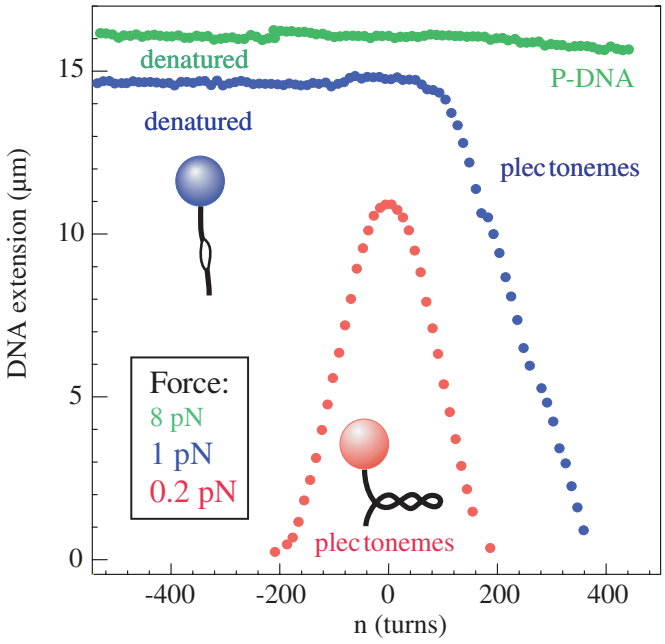

Figure 3. The response of DNA to supercoiling: variation of a molecule's extension versus the number n of extra turns applied to the molecule. At low force ($F = 0.2$ pN; red points), the extension curve is symmetric with a maximum at $n = 0$. The decrease in extension from the maximum is due to the molecule buckling to form plectonemes (twisted loops). At moderate forces ($F = 1$ pN; green points), buckling still occurs when positive turns are added. For negative supercoiling, denaturation bubbles appear and prevent loop formation. At high force ($F = 8$ pN; blue points), denaturation bubbles still occur for negative supercoiling, while a novel, denatured (43), and highly-twisted form of DNA [P-DNA (44)] is induced upon positive supercoiling; in both cases, the extension is nearly constant with added turns. Adapted from (22).

The mechanical response of a DNA molecule under constant force to a varying angular constraint n is shown in Figure 3, where n is the number of turns applied to the molecule. In order to compare the behavior of molecules having different lengths, it is useful to introduce the supercoiling density $\sigma = n/Lk_0$, where $Lk_0 = L/p$ is the number of helical turns in a relaxed DNA molecule of length L and p is the DNA helical pitch. The DNA extension is maximum when $n = 0$; as n increases, a torque builds up, the DNA pitch p changes slightly while the DNA's extension remains nearly constant. When n increases beyond a force-dependent critical point n_b, the DNA molecule buckles to form plectonemes, rather like the loops frequently seen in a garden hose or a telephone cord. These loops form for $|n| > |n_b|$ (i.e. the transition occurs at the same magnitude for both positive and negative added turns), causing the molecule's extension to shrink. At constant force, the size of each added loop remains constant; this leads to a linear reduction of the molecule extension with increasing $|n-n_b|$. Since the persistence length dictates DNA's bending radius, and thus that

of the loop, the extension shrinks by typically 50 nm per extra turn (41,42).

This description is very static; in fact DNA in water is subject to very strong Brownian fluctuations that smooth out the buckling transition. Thus, measured extension versus twist curves at low forces (Figure 3) present no sharp transition but rather a symmetric, round-topped 'mountain' shape with equal rising and falling slopes. This curve demonstrates that the molecule's extension is strongly sensitive to the angular constraint, at least on its rising and falling edge. Measuring the molecule's extension in real-time allows one to track minute changes in the supercoiling state of a DNA molecule.

At low forces (typically under 0.5 pN), the supercoiling behavior is symmetrical: the formation of plectonemes is not sensitive to the sign of the twist. As the stretching force is increased, so is the torque induced by twisting DNA, leading to structural changes in the molecule. In this high force regime, the twist stress now interacts with the chirality of the right-handed DNA helix. Unwinding a DNA molecule at high force opens a local denaturation bubble where the two DNA strands are no longer base paired, and do not wind around each other. This structural change alleviates the torsional stress to a constant level independent of n and prevents the occurrence of the buckling transition; thus the DNA extension does not shrink anymore [Figure 3; (43)]. Extreme overtwisting conditions (i.e. large positive torques) can also induce a structural transition to a new form of DNA called P-DNA (44).

The knowledge of the mechanical and structural properties of DNA has proved to be useful in the design of new assays of protein activity, especially in the field of DNA–protein interactions, e.g. the study of helicases and translocases. Here we describe different examples from the literature that demonstrate how biologically relevant issues can be addressed using single molecule manipulation. First, we describe the unwinding activity of different helicases: *Escherichia coli* UvrD, Hepatitis C virus NS3 and bacteriophage T7 gp4 helicases (within the T7 replication fork). Then we report on experiments probing the activity of two translocase: the *E.coli* Holliday junction migration protein RuvAB and FtsK, an *E.coli* protein involved in chromosome-segregation.

INDUCING A HOLLIDAY JUNCTION BY TWISTING A SINGLE MOLECULE

With magnetic tweezers, it is possible to explore the structure of DNA substrates with particular sequences. For example, one can pull on a DNA molecule that is palindromic, a property that confers upon the molecule the ability to adopt a cruciform structure with a Holliday junction at its center (45). This structure mimicks the typical intermediates encountered in the cell during homologous recombination. However, at low pulling force and when little rotation is applied, the palindromic molecule behaves as a normal DNA molecule, with no Holliday junction formation: rotating the bead induces plectoneme formation which is detected through a characteristic shortening of the molecule (Figure 4, green curve).

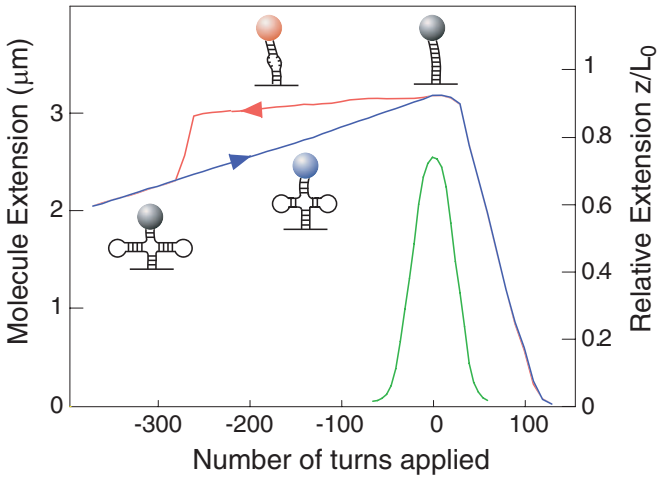

Figure 4. Extension versus supercoiling of a palindromic DNA molecule. The low force curve (green curve, F = 0.28 pN) is indistinguishable from the one observed when twisting a non-palindromic DNA molecule. Negatively supercoiling the substrate at moderate force (red curve, F = 1.45 pN) first induces denaturation with no noticeable change in the extension. The abrupt decrease in extension at about −260 turns is due to the formation of a Holliday junction in the molecule. Once the cruciform is formed, each subsequent negative turn leads to the migration of the junction by one helical turn, reducing the length of the vertical helix and lengthening each horizontal arm of the cruciform. The resulting slope (∼3 nm per added turn) reflects the helical pitch of dsDNA (see text). Once the Holliday junction is formed, the migration can be reversibly driven back and forth. Finally, when the negative supercoiling is gradually removed (blue curve, F = 1.45 pN), the extension rises linearly, reaching full length upon resorption of the junction when all the induced twist is relaxed. Adapted from (45).

The Holliday junction is most efficiently obtained by inducing first the formation of denaturation bubbles. As described above, this is simply done by untwisting the DNA while applying a moderate force (Figure 4, red curve; $F = 1.45$ pN): the length of the molecule does not significantly change in the negative supercoiling regime, since the untwisting is relaxed by denaturation bubbles. However, at some point the extension of the underwound molecule jumps to a shorter value resulting from the formation of a Holliday junction. The curve then displays a small, linear variation of extension with a slope of ∼3 nm per turn. This value is simply understood: for each extra negative turn applied to the bead, the Holliday junction reversibly exchanges one net turn of DNA helix from its vertical branches to its horizontal ones. If the molecule were fully stretched, the extension shrink would have been of one helical pitch $p = 3.6$ nm. However, due to Brownian fluctuations, the conformation of the branches deviates from the straight line, resulting in a reduced apparent shrinking of ∼3 nm/tr (45). In absence of divalent ions, the junction migrates smoothly upon rotations applied to the bead. In presence of magnesium, the stacking of the junction is stabilized and its migration is hindered (45).

Once extruded, the cruciform structure remains stable as long as a sufficient torsional constraint is applied. Upon rewinding the molecule, the junction dissociates as the molecule recovers its full extension (Figure 4, blue curve). Therefore, the curve displays a strong hysteretic behavior, which reflects the existence of the various metastable states and phase-space path-dependent behavior of the system.

CASE STUDIES

Helicase assay on a nicked DNA molecule reveals strand switching activity of UvrD

Helicases are enzymes that convert dsDNA to ssDNA. UvrD is an *E.coli* superfamily 1 helicase involved in DNA repair. It loads onto a nick and starts unwinding DNA in the 3′–5′ direction, relative to the strand on which it translocates.

Measuring this activity with magnetic tweezers is simple: Once a nicked DNA substrate is tethered between the flow cell glass surface and a magnetic bead, a stretching force is applied to the DNA molecule, the helicase and ATP are added, and the DNA extension monitored. The signature of helicase activity depends on the difference in elasticity between ssDNA and dsDNA: as described before, the extensions of ssDNA and dsDNA are equal at 5 pN; for higher forces, ssDNA is longer, while the reverse occurs at lower force. Since the helicase converts dsDNA to ssDNA, one then expects helicase activity to lengthen the DNA molecule at high force, and shorten it at low force. Indeed, this is exactly what is observed. However, it is much simpler to analyze the data taken at high force, (where the noise from Brownian fluctuations of the bead is less and immediate renaturation of the unwound strands is impeded), so we shall concentrate on this regime.

UvrD activity was observed at a stretching force of ~30 pN (25). Unwinding events appear as well-defined bursts of length increase in the DNA's extension time traces (Figure 5A). At low UvrD concentration ([UvrD] = 0.25 nM), bursts are well-separated, a signature that each of them is the result of the action of a single enzyme. Two populations of bursts are observed: the first displaying a fast falling edge (Figure 5A), the second a slow falling edge (Figure 5B).

Bursts from the first family are composed of a rising edge, corresponding to the gradual conversion of dsDNA into ssDNA due to helicase activity, followed by a fast falling edge, due to the quick rehybridization of the separated DNA strands upon dissociation of the UvrD–DNA complex. The shapes of these bursts give access to precious information on UvrD kinetics: the rising edge linear increase in length displays a relatively uniform velocity V_u = 35 nm/s

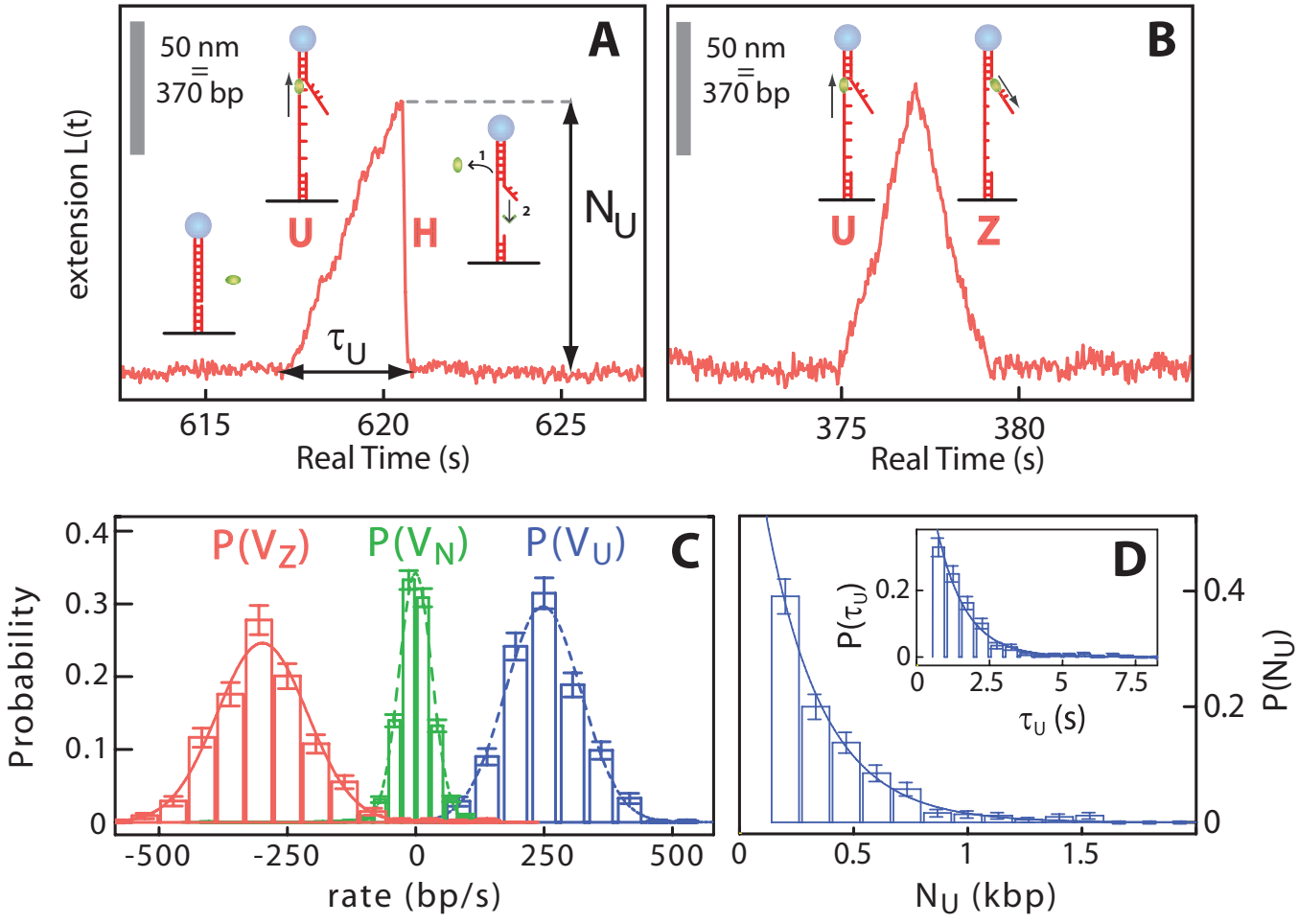

Figure 5. UvrD unwinding a nicked dsDNA stretched at 35 pN. (**A**) The molecule extension displays a burst of unwinding with a rising edge (U) with a constant rate (V_U) and an abrupt falling edge (H) associated with the rapid rehybridization of the dsDNA after the helicase dissociates from its substrate. (**B**) Second type of burst displaying a falling edge (Z) with a rate V_Z nearly opposite that of the rising edge. (**C**) Histogram of UvrD rates (V_N corresponds to the baseline noise signal between activity bursts). (**D**) Histograms of the amplitude of the bursts in number of base pairs unwound, N_U, and in duration, τ_U. All experiment done in [ATP] = 0.5 mM, [UvrD] = 0.25 nM. Adapted from (25).

that can be readily translated into base pairs: for each base pair unwound, the length increases by the extension difference between ssDNA and dsDNA, which is 0.135 nm at $F = 35$ pN. Thus, from the velocity of increase in extension, one can directly obtain the velocity of UvrD along the DNA substrate (Figure 5C): $V_u = 248 \pm 3$ bp/s (at saturating ATP concentration). In these conditions, the burst durations are Poisson-distributed with an average time $\langle \tau_u \rangle = 0.98 \pm 0.05$ s. The Poisson distribution indicates that UvrD has a constant probability to dissociate from its substrate. Due to the uniformity of velocity, this also leads to a Poisson distribution of the extent of DNA unwound with a characteristic number of bases unwound of $\langle N_u \rangle = 240 \pm 14$ bp (Figure 5D).

Bursts from the second family are obtained in 65% of the cases. Whereas their rising edge unwinding activity is indistinguishable from the first family, the falling edge has a much slower velocity, $V_z = -298 \pm 3$ bp/s (Figure 5B), that displays the same ATP dependence as the unwinding rate V_u (Michaelis–Menten kinetics of order one; $k_M = 53$ μM). This suggests that the slow falling edge corresponds to UvrD switching strands and thus propagating in the opposite direction. While the enzyme needs to perform mechanical work to initially unwind the DNA, after switching strands, it is pushed by the fork rezipping in its wake, which explains why $|V_z| > |V_u|$ by 17%.

What is the biological role of the strand switching behavior? How it could modulate UvrD activity in the nucleotide excision repair pathway is not clear. However, recent genetic experiments demonstrate that UvrD is involved in replication fork restart (46), probably through clearing the fork of bound RecA protein (47). One could speculate that switching strands could increase the efficiency of RecA removal, or participate in the initiation of the resolution of the stalled replication fork. Further experiments are needed to address these possible mechanisms.

The spatial resolution of the helicase experiment depends upon time averaging; it is typically 1 nm (corresponding to ~7 bp, using the 0.135 nm/bp factor for the conversion of dsDNA into ssDNA at 35 pN) for a signal averaged over 1 s. Since UvrD translocates by 35 nm during 1 s, it is impossible to detect in the real-time signal the enzymatic stepsize. However, as can be seen on Figure 5A, the leading edge of the unwinding burst presents a well-defined average velocity but also significant fluctuations. These fluctuations are larger than those observed in the signal outside the bursts, and originate in the random time between two consecutive steps. Statistical analysis of these fluctuations was shown to allow for an estimate of the step size (48–50). Applying this method gives a step size of 6 bp for UvrD, in good agreement with the estimate of Ali *et al.* in a single-turnover unwinding assay (51). This value significantly differs from the 1 bp per ATP hydrolyzed found by Dillingham *et al.* (52) on PcrA, a helicase which shares extended homology with UvrD. Two possible reasons could account for this discrepancy: first, the two enzymes could unwind DNA with different mechanisms; second, the statistical method used in (25) accumulates the fluctuations of enzymatic activity over time and several different enzymes, thus being subjected to respectively dynamic and static disorder (53). The models used to fit single-turnover data (51,52) relie on similar assumptions as the single molecule analysis and thus the step size calculation could be subjected to this caveat.

RNA unwinding by HCV NS3 helicase

Hepatitis C Virus helicase NS3 is able to catalyze the unwinding of both DNA and RNA duplexes. It is essential for viral replication (54–57). NS3 is a member of the superfamily 2 and has been shown to unwind RNA duplexes with a 3′–5′ polarity. In an optical tweezers based experiment, Dumont and coworkers (26) tethered the two ends of a RNA hairpin in an unzipping configuration (Figure 1B), in order to study the RNA unwinding activity of NS3. In this experiment, unwinding by the helicase resulted in an increase in the length of the handles. The 2 bp resolution of the experiment allowed for the observation of the step size of the enzyme, yielding insight on the enzymatic cycle.

Under the range of forces, ATP concentrations and RNA substrate sequences explored, NS3 helicase activity appeared as processive events corresponding to the opening of a 60 bp hairpin, suggesting a succession of steps of ~11 ± 3 bp separated by pauses. The pause duration increased upon decreasing the ATP concentration. Fitting of the variation of the pause duration against ATP concentration suggests a two step mechanism for pause exit, one of which depends on ATP binding. Unexpectedly, the stepping rate, i.e. the rate separating two successive pauses, appeared also to depend on ATP. Further investigations revealed that the steps are made up of three substeps, which size vary between 2 and 5 bp.

This step size value differed from the 18 bp value obtained in previous quenched flow experiments (58). The authors point out that this discrepancy might be due to a difference in the oligomeric state of the active enzyme: whereas bulk experiments typically preload the enzyme on its nucleic acid substrate, thus allowing dimerization, this is not the case in the single molecule experiment, and thus monomer activity may be observed. One should also note that a different value of 9 bp was obtained in bulk experiments on monomers of the NS3 helicase domain unwinding DNA (59). Another question raised by the step size measured in the single molecule experiments is its variability: typical deviations from the average of 3 bp are observed, much greater than the experimental noise (1 bp). This could be due to different factors, such as weak contact of RNA-binding domains in NS3, sequence effects, or coupling of the helicase stepping with RNA fraying.

NS3's stepping rate was insensitive to force, whereas the processivity was found to strongly increase with force, from an average value of 18 bp unwound at 5 pN to 53 bp unwound at 17 pN. Since the processivity did not depend on the ATP concentration, force must increase the time the enzyme remained bound to its substrate. The ATP dependence of the stepping rate displayed a first order Michaelis–Menten rate with the maximum unwinding rate of 51 bp/s and $k_M = 93$ nM.

Based on these results, the authors devised a model where translocation is accomplished by two different units, the first one in front binding to dsRNA (termed the translocator) and performing 11 bp steps, and the second one at the back (the helix opener) moving by steps of 2–5 bp. The force

independence of the unwinding rate suggests that the enzymatic cycle is not limited by RNA unwinding but rather by translocation.

Observation of unwinding and backsliding by RecBCD helicase

E.coli RecBCD is a helicase/nuclease involved in DNA repair (60,61). The enzyme loads preferentially on blunt ended dsDNA, from which it translocates and unwinds the duplex. DNA unwinding is accompanied by DNA degradation, preferentially on the 3′-terminated strand. Upon encountering a specific sequence termed χ, the enzyme switches the polarity of DNA cleavage and gains the ability to load RecA protein to initiate homologous recombination. Previous single molecule assays (8,9,12) without the application of force, discussed in (11), have shown that RecBCD is a rapid, highly processive motor capable of unwinding 30 kb before dissociating. In addition, the χ sequence induces a short pause, followed by further translocation by the enzyme, but with reduced rate.

By tethering a DNA molecule between a membrane-bound RecBCD enzyme and an optically trapped bead, Perkins *et al.* (24) could record the activity of the enzyme against an applied force (Figure 1D). As the enzyme translocates on and unwinds DNA, the length of the tether decreases, and the force is kept constant using a feedback loop. The DNA substrate used does not contain the χ sequence, to exclude any χ-induced switch of activity. However, even in the absence of its recognition sequence, short pauses are frequently observed (mean duration: 3 s, mean frequency: 0.14 s^{-1}), independently of [ATP] and force. Interestingly, the application of force occasionally induced episodes of reverse motion, i.e. backsliding of the enzyme. Sequences of backsliding could be followed by the rescue of forward translocation upon releasing the force to a lower value (0.5 pN). Backsliding motion seems to largely originate from the force, and not to be dominated by the catalysis of a chemical reaction, as the maximum backsliding rate is proportional to the force.

DNA elasticity could be exploited to analyze the tether resulting from backsliding motion. It appears that the persistence length of the tether is significantly lower than that of dsDNA, indicating that a significant portion of the tether is constituted of ssDNA. This finding indicates that unwound dsDNA is not immediately degraded by the nuclease subunit of the enzyme, but rather forms ssDNA loops.

Finally, it should be noted that both static and dynamic disorder were observed on RecBCD: first, the rate and force-dependence of the rate significantly differed from one molecule to the other. Second, a given enzyme could display successive interval of nearly constant rate translocation, and the variability of the rates observed between intervals could not be solely explained by stochastic stepping of the enzyme.

DNA unwinding within a moving replication fork

Lee and coworkers (33) have developed an assay based on extending a dsDNA molecule with a flow. This method was used to reconstitute the DNA replication fork: a forked DNA substrate was tethered by the lagging strand to the bottom of the flow cell and by the duplex to a bead, leaving the leading strand free. It was thus possible to study the replication complex of T7 bacteriophage (Figure 1A), which consists first of T7 gp4 helicase/primase, a DnaB-like hexameric, donut-shaped enzyme, which translocates 5′ to 3′ on the lagging strand, while displacing the leading strand (62). Its primase domain generates the ribonucleotides primers required for lagging strand DNA synthesis. However, it should be noted that the exact stoichiometry of the active form of gp4 *in vivo* is still debated: whereas electron microscopy data suggest a hexameric form of the enzyme (63), it was recently crystallized as a heptamer (64). In addition, work on the related *E.coli* replisome suggest that stoichiometric variability might play a role in the primosome mechanism (65,66), which might also be the case in the T7 context.

In the replication fork, gp4 is associated with the gp5-trx polymerase and the ssDNA binding protein gp2.5. This system is an attractive model to study how helicase activity is synchronized to other activities of the replication machinery.

In a first version of the assay, only the leading strand polymerase was added to the helicase. The buffer contained no ribonucleotides, thus inhibiting the priming activity of gp4. The leading strand polymerase-dependent synthesis of the complementary strand prevented rehybridization of the two strands behind the helicase. The elasticity difference between ss- and dsDNA was again used here: in the range of forces used (below 5 pN), the helicase-induced transformation of ds- into ssDNA resulted in a shortening of the molecule (Figure 6A and B). The polymerase activity cannot be directly measured, since it only affects the length of the (untethered) leading strand. The helicase–polymerase complex displays a processivity of ∼17 kb, a value much higher than the processivities of the helicase or polymerase alone (67), whereas the measured rate (∼160 bp/s) compares well with bulk measurements (68).

The addition of ribonucleotides in solution enables priming activity by gp4 (Figure 6C). Priming activity generated pauses in the traces showing the progression of the helicase–polymerase complex, whose distribution on the template sequence is in agreement with the location of the priming recognition sequences. The pause duration displays an exponential distribution with an average of ∼6 s.

Finally, adding excess polymerase in the reaction chamber allowed for the binding of the lagging strand polymerase, thus mimicking a full replication complex, with the exception of gp2.5. The primase-induced pauses were still observed, with a similar average duration. The pauses, corresponding to primer synthesis, are then followed by Okazaki fragment synthesis.

During this phase, the decrease in length was due to two contributions: dsDNA unwinding by the helicase (growing a loop between the helicase and the lagging strand polymerase), and backwards dsDNA synthesis by the lagging strand DNA polymerase (Figure 6D). It appeared from the analysis of the time traces that the rate of the lagging strand DNA polymerase is similar to the leading strand one. Upon release of the replication loop on the lagging strand, the DNA molecule abruptly extends by the length of the Okazaki fragment loop (Figure 6E). This study provides a possible mechanism for the synchronization of leading and lagging

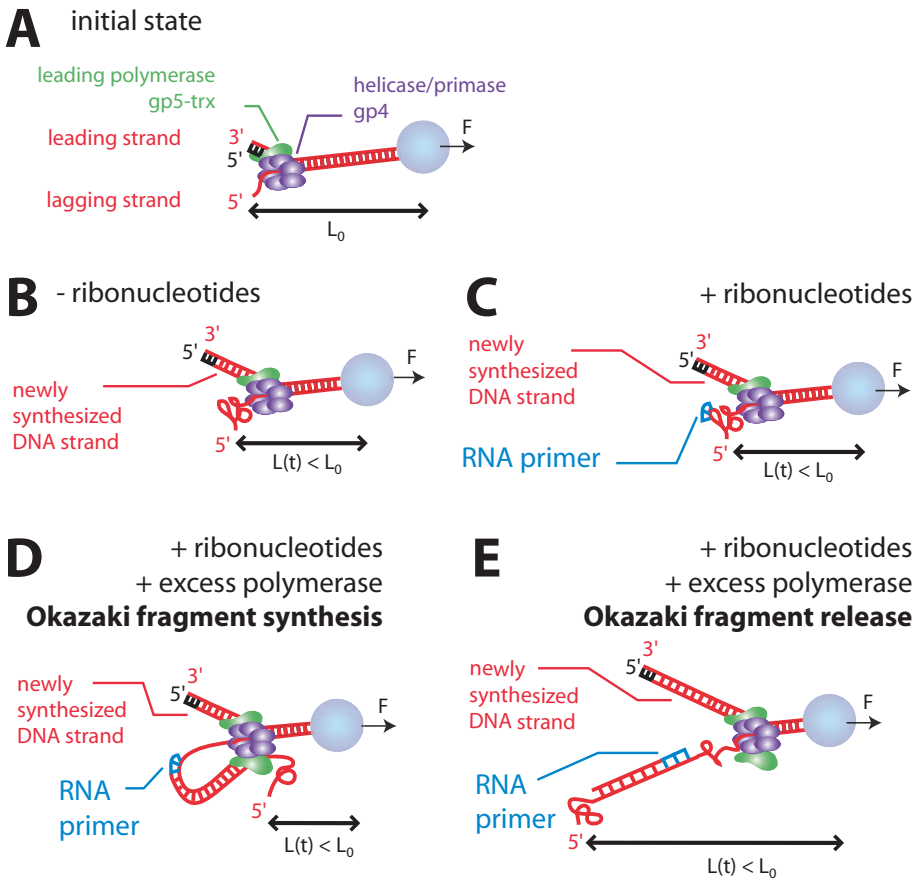

Figure 6. Schematic description of the T7 replication fork experiment (33). (**A**) A partial replication complex composed of the helicase/primase and the leading strand polymerase is preloaded on the forked DNA substrate. (**B**) In a first version of the assay, the helicase unwinds dsDNA into ssDNA, while DNA polymerase synthesizes the leading complementary strand. ssDNA generation results in a shortening of the molecule in the range of forces explored ($F \sim 3$ pN). (**C**) Addition of ribonucleotides to the solution triggers sporadic priming by gp4, which can be observed as pauses in the tether length decrease. (**D**) Addition of excess DNA polymerases allows for lagging strand DNA synthesis after priming by gp4. The tether length still decreases as a result of the formation of a loop between the helicase and the lagging strand polymerase. (**E**) Okazaki fragment release generates an abrupt lengthening of the tether.

strand DNA synthesis: the whole replication complex halts while the primer synthesis proceeds. The molecular details of the enzymatic coupling lying behind the replication fork halting still remain to be explored.

Holliday junction migration induced by RuvAB

Homologous recombination is a fundamental and highly conserved mechanism of genetic exchange between two homologous DNA molecules. It is initiated by a strand exhange between the two dsDNA molecules, forming a four-way branched DNA structure termed Holliday junction. In the absence of protein or mechanical constraints, the branch point of a Holliday junction can diffuse into the sequence by a random walk process in which one step corresponds to the exchange at the branch point of 1 bp between the arms of the cruciform structure. However, *in vivo*, cells need to control precisely the fate of the Holliday junction, and consequently the direction, the velocity and the range of branch point migration (69). In *E.coli*, the RuvA, RuvB and RuvC proteins process the Holliday junction intermediate toward the formation of two recombinant DNA molecules. The RuvAB complex binds specifically to the cruciform structure and induces the strand exchange in the direction determined by the orientation of its loading on the Holliday junction. RuvC is responsible for the resolution of the branched intermediate in two independent dsDNA molecules. RuvC-mediated resolution occurs preferentially at consensus sequences: 5′-(A/T)TT(G/C).

The activity of RuvAB can be measured with a magnetic tweezer using a cruciform DNA substrate (23,27). In such experiments, the DNA substrate consists of an almost entirely palindromic molecule, displaying a pre-formed Holliday junction in its center. Small regions of heterology flank the initial branch point position to prevent total migration of the lateral arms or spontaneous diffusion of the branch point (Figure 7A).

Once the DNA cruciform substrate is tethered by a magnetic bead, and RuvA and RuvB have been added in the flow cell, the migration activity of the RuvAB complex is measured directly by monitoring the extension variation of the molecule. It has been observed that the complex is highly processive: being able to continuously exchange at least 6–7 kb of the DNA substrate. Once the end of the homologous region is reached, the strand exchange may stop and, after a while, proceed in the reverse direction, resulting in a

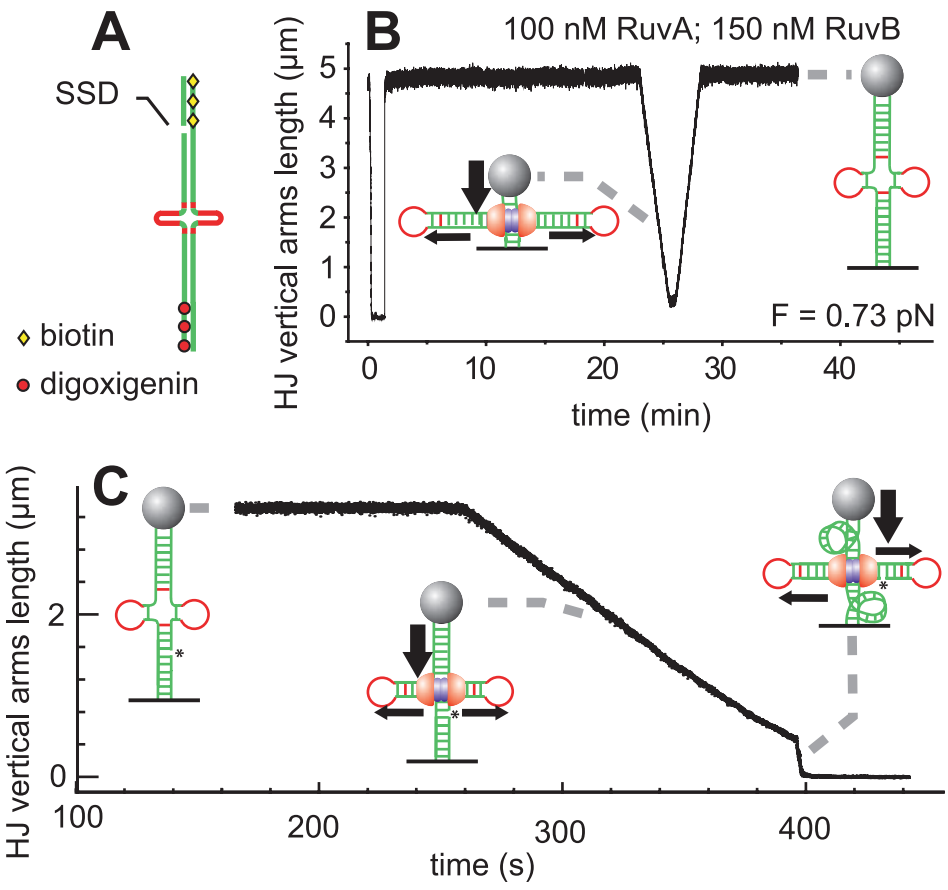

Figure 7. Holliday junction migration induced by RuvAB. (**A**) Molecule design used in Ref. (23). Sequence heterologies are shown in red. Everywhere else, the sequence is palindromic (green) to enable homologous strand exchange. A single-strand discontinuity (SSD) relaxes any rotational constraint that could result from the multiple biotin or digoxygenin labelling at the molecule extremities. (**B**) Typical burst of RuvAB activity. A total of 20 min after RuvAB has been injected in the capillary, the molecule extension is smoothly driven to nearly zero; in less than a minute the motion reverses and drives the molecule back to full extension. (**C**) Holliday junction migration by RuvAB on a molecule containing a nick (marked by a star) 0.5 micron from the ends. When the extension exceeds 0.5 micron, the burst is similar to (B) (extended time scale): the junction migrates smoothly and all induced rotation is liberated by the nick. Beyond 0.5 microns, the nick is transferred to the horizontal arms and the supercoiling induced by Holliday junction migration cannot be relaxed anymore. This produces plectonemes which drastically reduce the molecule extension. Experiments were performed in the presence of 1 mM ATP, an ATP regenerating system, 100 nM RuvA, and 200 nM RuvB. Adapted from (23).

re-lengthening of the molecule. The waiting time before reversal decreases if the concentration of RuvB is increased from 150 to 670 nM, suggesting that at least a partial dissociation of the complex is required to initiate backwards migration. However, increasing the RuvB concentration also results in a destabilization of the migration activity (frequent pauses are observed, as well as early reversals and irregularities in the migration speed), illustrating possible interactions of the migrating complex with RuvB proteins free in solution or bound along the DNA arms. It is interesting to note that the presence of RuvC consensus sequences does not seem to affect the RuvAB complex migration, supporting the picture of RuvC being part of a RuvABC complex, rather than RuvAB dissociating to allow RuvC binding in the process of resolving the recombinational intermediate.

Concerning the migration speed, magnetic tweezers experiments, along with TPM techniques [(70), see (11) for a discussion] have found essentially identical results: ~50 bp/s at 37°C (the apparent factor two in the result of Ref. (23) comes from a different convention for the definition of the speed (J. Stavans, personal communication)]. Also the migration rate of RuvAB has been found to display abrupt changes between a small number of discrete values (23), possibly indicating that not all the subunits of the RuvB hexameric ring are functionally equivalent.

The back and forth migration activity of RuvAB allowed measurement of the effect of a force that either hinders or assists the migration: a hindering (assisting) force is defined to be negative (positive), and occurs when migration shortens (lengthens) the molecule. The RuvAB complex activity appears to be essentially force independent up to 15 pN and is able to work against external forces up to 23 pN (23).

For each DNA helical turn transferred from the vertical arms to the horizontal ones, one negative linking number unit is absorbed in order to unwind the double helix. When the DNA molecule is nicked on its vertical arm, this supercoil induction does not generate any torsional constraint. However, during long events the RuvAB complex may induce the migration of the branch point through the (specifically

introduced) nick. In this case, the nick passes to one of the horizontal arms, becoming ineffective in relaxing the torsional constraints, and the molecule suddenly loses its rotational freedom. This means that the global linking number of the DNA molecule is fixed, and that each negative supercoil absorbed by the unwinding of the vertical arms must be compensated for by a positive supercoil induced in these arms. As RuvAB translocates beyond the nick location, the positive supercoils induced in the vertical arms generate plectonemes that add a contribution to the extension decrease (typically 50 nm for every 10.5 bp traveled instead of 3.6 nm). This causes a sharp acceleration in the time trace that marks the position of the nick. Despite the presence of plectonemes, the migration rate of the branch point in a supercoilable molecule can still be measured. From the properties of a supercoilable DNA molecule, one knows how the extension of the molecule reduces when it is positively supercoiled. This plectoneme-induced decrease in extension ($p \approx 50$ nm/tr—dependent on the force) superimposes upon the strand exchange-induced decrease ($h \approx 3$ nm/tr—dependent on the relative extension of the molecule, and thus also on the force). Therefore, in the presence of plectonemes, the strand exchange-induced extension variation v_0 can be deduced by correcting the apparent extension variation rate v: $v_0 = v/(1 + p/h)$. The factor $(1 + p/h)$ is typically of the order of 10 to 20 depending on the force level. Experimentally, it is found here that the branch point migration speed is roughly the same with or without plectonemes, since the ratio v_0 with *vs.* v_0 without has the value $(1 + p/h)$.

FtsK: slowly inducing supercoils

Motors tracking on an helical filament like DNA or actin, may rotate around the filament if the step size of the motor is not a multiple of the helical pitch of the filament. This fact has been checked for Myosin V (71). In the case of DNA, enzymes that track one of DNA's two strands, such as helicases or RNA polymerase, rotate relative to the DNA by one turn per helical pitch traveled. However, some DNA motor proteins, such as the bacterial cell division protein FtsK, are truly double-stranded translocases. In this case the amount of relative rotation is not obvious, and will depend on the details of the protein's translocation mechanism. Magnetic tweezers, with their unique ability to both manipulate and detect the supercoiled state of a DNA molecule, provide a mean to investigate this problem: translocation will cause quantifiable changes in the amount of supercoiling if the motor protein is immobilized.

In particular, the action of FtsK is considered here: previous experiments utilizing nicked DNA molecules had shown that single FtsK complexes are capable of extruding loops of DNA [Figure 8B; (29,30)]. Loop extrusion involves a single protein complex that contacts the DNA in two places: a 'mobile' contact where translocation occurs, and an 'immobile' contact that defines the loop. In a magnetic tweezer, loop extrusion on a nicked DNA molecule is measured as a constant-velocity decrease in DNA extension that directly corresponds to the translocation velocity of the motor. This velocity is extraordinarily high: in saturating ATP conditions, FtsK typically travels at 7000 bp/s (2.4 μm/s; compare 35 nm/s for UvrD), and, at low stretching forces, typically travels several kilo-base pairs per translocation event. These events can end either with the protein unbinding, or with a reversal of the translocation direction (in which the bead rises back up at a similar velocity to the initial decrease) in a manner reminiscent to the reversals described above for both RuvAB and UvrD.

This behavior changes in a subtle, but important, fashion when a coilable (i.e. not nicked) DNA molecule is used. Now, the DNA is sensitive to changes in supercoiling, and since FtsK's immobile contact serves to rotationally fix the protein complex, all relative rotation between DNA and FtsK will be absorbed by the DNA. As described above, this twisting of a single DNA molecule can add or remove plectonemes, altering the DNA's end-to-end length. These properties were used here to study the link between translocation and rotation for FtsK. The experiment is carried out by adding negative supercoils to a single DNA molecule at low forces, so that it contains many (20–60) negative plectonemes that decrease the DNA's extension. When FtsK is added, protein complexes bind the DNA, and begin to extrude loops. Loop extrusion alone tends to decrease the DNA's extension (Figure 8B); however, simultaneously, the DNA is absorbing the relative rotation of the translocating motor. These induced supercoils are positive in polarity in advance of the translocating motor, thus they annihilate the existing negative plectonemes (note that an equal number of negative supercoils are induced behind the motor, into the extruded loop, but these are not detectable). The length of DNA in each annihilated plectoneme is liberated, tending to increase the measured extension. Indeed, measured events in these conditions show an initial increase in extension, indicating that the plectoneme removal effect is greater (at least initially) than the loop extrusion effect (Figure 8C).

A simple calculation allows one to relate the height of this increase to the rate of supercoil induction by the translocating FtsK motor (31). Interestingly, this calculation indicates that FtsK induces ~0.07 supercoils per DNA helical pitch traveled, i.e. over 10 times less than what one would expect if FtsK tracked one strand of the DNA. For example, compare the result discussed above on the effect of supercoil induction by RuvAB: in that case, the motor protein induced 1 supercoil per pitch traveled. FtsK's slow supercoil induction rate is the first direct evidence of a DNA motor protein that does not directly follow DNA's groove, a discovery that raises the question of how exactly FtsK interacts with the DNA while translocating. While the molecular mechanism of translocation is not yet clear, the advantage to the cell of such a low rate of supercoil induction is more obvious: *in vivo*, FtsK is involved in the transport of chromosomes whose supercoiling density is tightly controlled by the cell. FtsK's low rate of supercoil induction undoubtedly helps by not perturbing that density; in fact, the rate of 0.07 supercoils per pitch is intriguingly close to the ideal value that would cause no change to the chromosome's topology (31).

CONCLUSION

In this review, we have described how precision measurements of DNA's mechanical properties can be exploited to investigate DNA–protein interactions. For brevity, we have not detailed the various fluorescent techniques that have

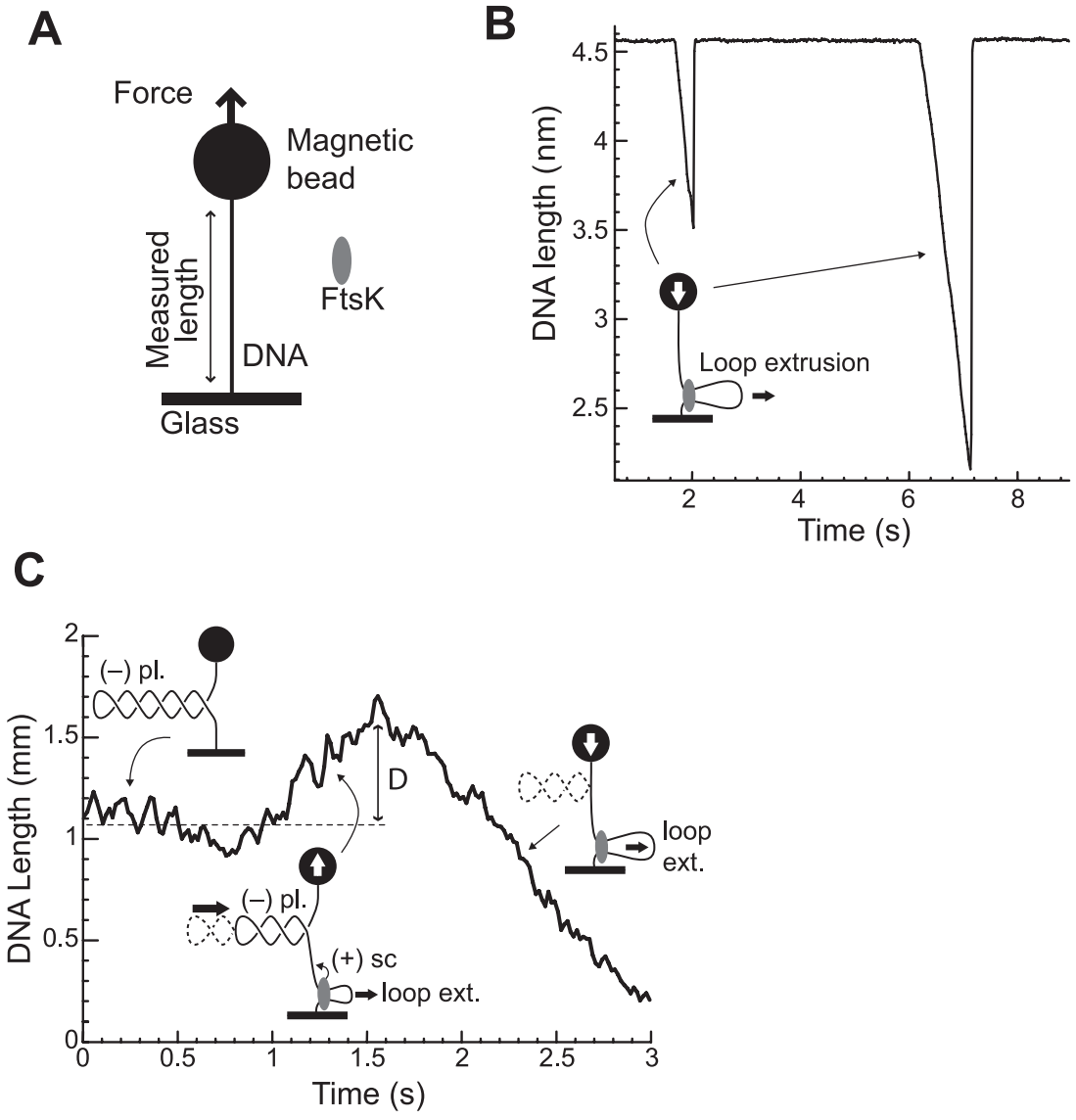

Figure 8. (**A**) Geometry of the magnetic tweezer experiment with FtsK. (**B**) Activity of FtsK on a nicked DNA molecule. Upon binding DNA, FtsK begins to extrude a loop, decreasing the measured DNA extension at a constant-velocity. (**C**) Activity of FtsK on a DNA molecule that initially contains negative plectonemes (pl.). As before, FtsK extrudes a loop upon binding the DNA. However, now the relative rotation between the enzyme and the DNA induces positive supercoils that remove the negative plectonemes. This effect tends to increase the bead height, as seen in the experimental trace, and continues until all plectonemes have been removed. At this point, the DNA length decreases due to loop extrusion alone, as in (A). Figure adapted from Refs. (29,31).

been used to study helicases, such as Rep (6,7,10) and RecBCD (5,8,9) and translocases, such as Rad54 [See S.C. Kowalczykowski contribution, and (11) for a review), by monitoring the fluorescence of labeled proteins and/or DNA on a substrate that is significantly fluctuating (e.g. a DNA stretched by a flow). Although these techniques have a somewhat limited spatial resolution, they offer real-time visualization of the enzyme's activity on DNA.

The present work can be extended in two directions: using similar techniques to measure other proteins, and developing novel analogous techniques. The former path is fairly straightforward: since each of the enzymes we have described is representative of a much larger class of motor proteins, it is clear that these techniques can be usefully applied to determine the characteristics of many other proteins. Secondly, there are many possibilities for developing novel techniques. For example, the flexibility of DNA's base pairing allows, relatively easily, the design of many different DNA structures, such as the Holliday junction structures we have already described. This ability represents an opportunity for the creative researcher to design novel DNA structures (hairpins, etc.) that interact with proteins in specific ways. One could imagine studying stalled replication forks utilizing three way junctions and the enzymes involved in restarting the process. Another direction for improvement of the technique of these types of experiments is in the micromanipulation technique itself. The current precision of the measurement of DNA extension (a few nm) is just slightly greater than the typical motor protein step sizes (a few bp $\sim$1 nm); thus with a small increase in resolution, individual steps will be visible, giving a great deal of insight into proteins' structural and enzymatic properties (72). Finally,

as seen in some recent single molecule experiments, the integration of real-time measurement and manipulation of DNA length, as described here, with the directness of fluorescence imaging techniques will greatly extend the power and diversity of single molecule measurement techniques.

ACKNOWLEDGEMENTS

The authors thank our collaborators on the presented works: T.R. Strick, M.N. Dessinges, B. Maier, X.G. Xi, K. Neuman, H. Yokota, M. Grigoriev. This work was supported by grants from CNRS, ANR, ACI DRAB CNRS program, ARC and the EEC under the 'MolSwitch' program. Funding to pay the Open Access publication charges for this article was provided by CNRS.

Conflict of interest statement. None declared.

REFERENCES

1. Delagoutte,E. and von Hippel,P.H. (2002) Helicase mechanisms and the coupling of helicases within macromolecular machines. Part I: Structures and properties of isolated helicases. *Q. Rev. Biophys.*, **35**, 431–478.
2. Delagoutte,E. and von Hippel,P.H. (2003) Helicase mechanisms and the coupling of helicases within macromolecular machines. Part II: Integration of helicases into cellular processes. *Q. Rev. Biophys.*, **36**, 1–69.
3. Tuteja,N. and Tuteja,R. (2004) Prokaryotic and eukaryotic DNA helicases. Essential molecular motor proteins for cellular machinery. *Eur. J. Biochem.*, **271**, 1835–1848.
4. Tuteja,N. and Tuteja,R. (2004) Unraveling DNA helicases. Motif, structure, mechanism and function. *Eur. J. Biochem.*, **271**, 1849–1863.
5. Handa,N., Bianco,P.R., Baskin,R.J. and Kowalczykowski,S.C. (2005) Direct visualization of RecBCD movement reveals cotranslocation of the RecD motor after chi recognition. *Mol. Cell*, **17**, 745–750.
6. Ha,T., Rasnik,I., Cheng,W., Babcock,H.P., Gauss,G.H., Lohman,T.M. and Chu,S. (2002) Initiation and re-initiation of DNA unwinding by the *Escherichia coli* Rep helicase. *Nature*, **419**, 638–641.
7. Rasnik,I., Myong,S., Cheng,W., Lohman,T.M. and Ha,T. (2004) DNA-binding orientation and domain conformation of the *E. coli* rep helicase monomer bound to a partial duplex junction: single-molecule studies of fluorescently labeled enzymes. *J. Mol. Biol.*, **336**, 395–408.
8. Spies,M., Bianco,P.R., Dillingham,M.S., Handa,N., Baskin,R.J. and Kowalczykowski,S.C. (2003) A molecular throttle: the recombination hotspot chi controls DNA translocation by the RecBCD helicase. *Cell*, **114**, 647–654.
9. Bianco,P.R., Brewer,L.R., Corzett,M., Balhorn,R., Yeh,Y., Kowalczykowski,S.C. and Baskin,R.J. (2001) Processive translocation and DNA unwinding by individual RecBCD enzyme molecules. *Nature*, **409**, 374–378.
10. Myong,S., Rasnik,I., Joo,C., Lohman,T.M. and Ha,T. (2005) Repetitive shuttling of a motor protein on DNA. *Nature*, **437**, 1321–1325.
11. Rasnik,I., Myong,S. and Ha,T. (2006) Unraveling helicase mechanisms one molecule at a time. *Nucleic Acids Res.*
12. Dohoney,K.M. and Gelles,J. (2001) Chi-sequence recognition and DNA translocation by single RecBCD helicase/nuclease molecules. *Nature*, **409**, 370–374.
13. Schafer,D.A., Gelles,J., Sheetz,M.P. and Landick,R. (1991) Transcription by single molecules of RNA polymerase observed by light microscopy. *Nature*, **352**, 444–448.
14. Yin,H., Landick,R. and Gelles,J. (1994) Tethered particle motion method for studying transcript elongation by a single RNA polymerase molecule. *Biophys J.*, **67**, 2468–2478.
15. Moy,V.T., Florin,E.L. and Gaub,H.E. (1994) Intermolecular forces and energies between ligands and receptors. *Science*, **266**, 257–259.
16. Evans,E., Ritchie,K. and Merkel,R. (1995) Sensitive force technique to probe molecular adhesion and structural linkages at biological interfaces. *Biophys J.*, **68**, 2580–2587.
17. Cluzel,P., Lebrun,A., Heller,C., Lavery,R., Viovy,J.L., Chatenay,D. and Caron,F. (1996) DNA: an extensible molecule. *Science*, **271**, 792–794.
18. Ishijima,A., Doi,T., Sakurada,K. and Yanagida,T. (1991) Sub-piconewton force fluctuations of actomyosin *in vitro*. *Nature*, **352**, 301–306.
19. Neuman,K.C. and Block,S.M. (2004) Optical trapping. *Rev. Sci. Instrum.*, **75**, 2787–2809.
20. Gosse,C. and Croquette,V. (2002) Magnetic tweezers: micromanipulation and force measurement at the molecular level. *Biophys J.*, **82**, 3314–3329.
21. Strick,T.R., Dessinges,M.N., Charvin,G., Dekker,N.H., Allemand,J.F., Bensimon,D. and Croquette,V. (2003) Stretching of macromolecules and proteins. *Rep. Prog. Phys.*, **66**, 1–45.
22. Charvin,G., Allemand,J.F., Strick,T.R., Bensimon,D. and Croquette,V. (2004) Twisting DNA: single molecule studies. *Contemporary Phys.*, **45**, 383–403.
23. Dawid,A., Croquette,V., Grigoriev,M. and Heslot,F. (2004) Single-molecule study of RuvAB-mediated Holliday-junction migration. *Proc. Natl Acad. Sci. USA*, **101**, 11611–11616.
24. Perkins,T.T., Li,H.W., Dalal,R.V., Gelles,J. and Block,S.M. (2004) Forward and reverse motion of single RecBCD molecules on DNA. *Biophys J.*, **86**, 1640–1648.
25. Dessinges,M.N., Lionnet,T., Xi,X.G., Bensimon,D. and Croquette,V. (2004) Single-molecule assay reveals strand switching and enhanced processivity of UvrD. *Proc. Natl Acad. Sci. USA*, **101**, 6439–6444.
26. Dumont,S., Cheng,W., Serebrov,V., Beran,R.K., Tinoco,I.,Jr, Pyle,A.M. and Bustamante,C. (2006) RNA translocation and unwinding mechanism of HCV NS3 helicase and its coordination by ATP. *Nature*, **439**, 105–108.
27. Amit,R., Gileadi,O. and Stavans,J. (2004) Direct observation of RuvAB-catalyzed branch migration of single Holliday junctions. *Proc. Natl Acad. Sci. USA*, **101**, 11605–11610.
28. Saleh,O.A., Allemand,J.F., Croquette,V. and Bensimon,D. (2005) Single-molecule manipulation measurements of DNA transport proteins. *Chemphyschem.*, **6**, 813–818.
29. Saleh,O.A., Perals,C., Barre,F.X. and Allemand,J.F. (2004) Fast, DNA-sequence independent translocation by FtsK in a single-molecule experiment. *EMBO J.*, **23**, 2430–2439.
30. Pease,P.J., Levy,O., Cost,G.J., Gore,J., Ptacin,J.L., Sherratt,D., Bustamante,C. and Cozzarelli,N.R. (2005) Sequence-directed DNA translocation by purified FtsK. *Science*, **307**, 586–590.
31. Saleh,O.A., Bigot,S., Barre,F.X. and Allemand,J.F. (2005) Analysis of DNA supercoil induction by FtsK indicates translocation without groove-tracking. *Nature Struct. Mol. Biol.*, **12**, 436–440.
32. Bustamante,C., Chemla,Y.R., Forde,N.R. and Izhaky,D. (2004) Mechanical processes in biochemistry. *Annu. Rev. Biochem.*, **73**, 705–748.
33. Lee,J.B., Hite,R.K., Hamdan,S.M., Xie,X.S., Richardson,C.C. and van Oijen,A.M. (2006) DNA primase acts as a molecular brake in DNA replication. *Nature*, **439**, 621–624.
34. Smith,S.B., Cui,Y. and Bustamante,C. (2003) Optical-trap force transducer that operates by direct measurement of light momentum. *Meth. Enzymol.*, **361**, 134–162.
35. Bustamante,C., Marko,J.F., Siggia,E.D. and Smith,S. (1994) Entropic elasticity of lambda-phage DNA. *Science*, **265**, 1599–1600.
36. Bouchiat,C., Wang,M.D., Allemand,J., Strick,T., Block,S.M. and Croquette,V. (1999) Estimating the persistence length of a worm-like chain molecule from force-extension measurements. *Biophys J.*, **76**, 409–413.
37. Strick,T.R., Allemand,J.F., Bensimon,D. and Croquette,V. (2000) Stress-induced structural transitions in DNA and proteins. *Annu. Rev. Biophys Biomol. Struct.*, **29**, 523–543.
38. Dessinges,M.N., Maier,B., Zhang,Y., Peliti,M., Bensimon,D. and Croquette,V. (2002) Stretching single stranded DNA, a model polyelectrolyte. *Phys. Rev. Lett.*, **89**, 248102.
39. EssevazRoulet,B., Bockelmann,U. and Heslot,F. (1997) Mechanical separation of the complementary strands of DNA. *Proc. Natl Acad. Sci. USA*, **94**, 11935–11940.
40. Danilowicz,C., Coljee,V.W., Bouzigues,C., Lubensky,D.K., Nelson,D.R. and Prentiss,M. (2003) DNA unzipped under a constant force exhibits multiple metastable intermediates. *Proc. Natl Acad. Sci. USA*, **100**, 1694–1699.

41. Strick,T.R., Croquette,V. and Bensimon,D. (1998) Homologous pairing in stretched supercoiled DNA. *Proc. Natl Acad. Sci. USA*, **95**, 10579–10583.
42. Allemand,J.F., Bensimon,D., Lavery,R. and Croquette,V. (1998) Stretched and overwound DNA forms a Pauling-like structure with exposed bases. *Proc. Natl Acad. Sci. USA*, **95**, 14152–14157.
43. Strick,T.R., Allemand,J.F., Bensimon,D., Bensimon,A. and Croquette,V. (1996) The elasticity of a single supercoiled DNA molecule. *Science*, **271**, 1835–1837.
44. Strick,T.R., Allemand,J.F., Bensimon,D. and Croquette,V. (1998) Behavior of supercoiled DNA. *Biophys J.*, **74**, 2016–2028.
45. Dawid,A., Guillemot,F., Breme,C., Croquette,V. and Heslot,F. (2006) Mechanically controlled DNA extrusion from a palindromic sequence by single molecule micromanipulation. *Phys. Rev. Lett.*, **96**, 188102.
46. Flores,M.J., Bidnenko,V. and Michel,B. (2004) The DNA repair helicase UvrD is essential for replication fork reversal in replication mutants. *EMBO Rep.*, **5**, 983–988.
47. Flores,M.J., Sanchez,N. and Michel,B. (2005) A fork-clearing role for UvrD. *Mol. Microbiol.*, **57**, 1664–1675.
48. Charvin,G., Bensimon,D. and Croquette,V. (2002) On the relation between noise spectra and the distribution of time between steps for single molecular motors. *Single Mol.*, **3**, 43–48.
49. Neuman,K.C., Saleh,O.A., Lionnet,T., Lia,G., Allemand,J.F., Bensimon,D. and Croquette,V. (2005) Statistical determination of the step size of molecular motors. *J. Phys-Condens Mat.*, **17**, S3811–S3820.
50. Svoboda,K., Mitra,P.P. and Block,S.M. (1994) Fluctuation analysis of motor protein movement and single enzyme kinetics. *Proc. Natl Acad. Sci. USA*, **91**, 11782–11786.
51. Ali,J.A. and Lohman,T.M. (1997) Kinetic measurement of the step size of DNA unwinding by *Escherichia coli* UvrD helicase. *Science*, **275**, 377–380.
52. Dillingham,M.S., Wigley,D.B. and Webb,M.R. (2000) Demonstration of unidirectional single-stranded DNA translocation by PcrA helicase: measurement of step size and translocation speed. *Biochemistry*, **39**, 205–212.
53. Xie,X.S. and Lu,H.P. (1999) Single-molecule enzymology. *J. Biol. Chem.*, **274**, 15967–15970.
54. Dimitrova,M., Imbert,I., Kieny,M.P. and Schuster,C. (2003) Protein–protein interactions between hepatitis C virus nonstructural proteins. *J. Virol.*, **77**, 5401–5414.
55. Pang,P.S., Jankowsky,E., Planet,P.J. and Pyle,A.M. (2002) The hepatitis C viral NS3 protein is a processive DNA helicase with cofactor enhanced RNA unwinding. *EMBO J.*, **21**, 1168–1176.
56. Levin,M.K., Gurjar,M. and Patel,S.S. (2005) A Brownian motor mechanism of translocation and strand separation by hepatitis C virus helicase. *Nature Struct. Mol. Biol.*, **12**, 429–435.
57. Kim,J.L., Morgenstern,K.A., Griffith,J.P., Dwyer,M.D., Thomson,J.A., Murcko,M.A., Lin,C. and Caron,P.R. (1998) Hepatitis C virus NS3 RNA helicase domain with a bound oligonucleotide: the crystal structure provides insights into the mode of unwinding. *Structure*, **6**, 89–100.
58. Serebrov,V. and Pyle,A.M. (2004) Periodic cycles of RNA unwinding and pausing by hepatitis C virus NS3 helicase. *Nature*, **430**, 476–480.
59. Levin,M.K., Wang,Y.H. and Patel,S.S. (2004) The functional interaction of the hepatitis C virus helicase molecules is responsible for unwinding processivity. *J. Biol. Chem.*, **279**, 26005–26012.
60. Kuzminov,A. (1999) Recombinational repair of DNA damage in *Escherichia coli* and bacteriophage lambda. *Microbiol. Mol. Biol. Rev.*, **63**, 751–813.
61. Kowalczykowski,S.C., Dixon,D.A., Eggleston,A.K., Lauder,S.D. and Rehrauer,W.M. (1994) Biochemistry of homologous recombination in *Escherichia coli*. *Microbiol Rev.*, **58**, 401–465.
62. Patel,S.S. and Picha,K.M. (2000) Structure and function of hexameric helicases. *Annu. Rev. Biochem.*, **69**, 651–697.
63. Egelman,E.H., Yu,X., Wild,R., Hingorani,M.M. and Patel,S.S. (1995) Bacteriophage T7 helicase/primase proteins form rings around single-stranded DNA that suggest a general structure for hexameric helicases. *Proc. Natl Acad. Sci. USA*, **92**, 3869–3873.
64. Toth,E.A., Li,Y., Sawaya,M.R., Cheng,Y. and Ellenberger,T. (2003) The crystal structure of the bifunctional primase-helicase of bacteriophage T7. *Mol. Cell*, **12**, 1113–1123.
65. Thirlway,J., Turner,I.J., Gibson,C.T., Gardiner,L., Brady,K., Allen,S., Roberts,C.J. and Soultanas,P. (2004) DnaG interacts with a linker region that joins the N- and C-domains of DNAB and induces the formation of 3-fold symmetric rings. *Nucleic Acids Res.*, **32**, 2977–2986.
66. Corn,J.E., Pease,P.J., Hura,G.L. and Berger,J.M. (2005) Crosstalk between primase subunits can act to regulate primer synthesis in trans. *Mol. Cell*, **20**, 391–401.
67. Jeong,Y.J., Levin,M.K. and Patel,S.S. (2004) The DNA-unwinding mechanism of the ring helicase of bacteriophage T7. *Proc. Natl Acad. Sci. USA*, **101**, 7264–7269.
68. Stano,N.M., Jeong,Y.J., Donmez,I., Tummalapalli,P., Levin,M.K. and Patel,S.S. (2005) DNA synthesis provides the driving force to accelerate DNA unwinding by a helicase. *Nature*, **435**, 370–373.
69. West,S.C. (1997) Processing of recombination intermediates by the RuvABC proteins. *Annu. Rev. Genet.*, **31**, 213–244.
70. Dennis,C., Fedorov,A., Kas,E., Salome,L. and Grigoriev,M. (2004) RuvAB-directed branch migration of individual Holliday junctions is impeded by sequence heterology. *EMBO J.*, **23**, 2413–2422.
71. Ali,M.Y., Uemura,S., Adachi,K., Itoh,H., Kinosita,K.,Jr and Ishiwata,S. (2002) Myosin V is a left-handed spiral motor on the right-handed actin helix. *Nature Struct. Biol.*, **9**, 464–467.
72. Abbondanzieri,E.A., Greenleaf,W.J., Shaevitz,J.W., Landick,R. and Block,S.M. (2005) Direct observation of base-pair stepping by RNA polymerase. *Nature*, **438**, 460–465.
73. Maier,B., Bensimon,D. and Croquette,V. (2000) Replication by a single DNA polymerase of a stretched single-stranded DNA. *Proc. Natl Acad. Sci. USA*, **97**, 12002–12007.